A. Sundaramurthy
Department of Defense,
Biotechnology High Performance Computing
Software Applications Institute,
Telemedicine and Advanced Technology
Research Center,
U.S. Army Medical Research and Materiel
Command,
504 Scott Street,
Fort Detrick, MD 21702
e-mail: asundaramurthy@bhsai.org

M. Skotak
Department of Biomedical Engineering,
Center for Injury Biomechanics, Materials
and Medicine,
New Jersey Institute of Technology,
University Heights,
Newark, NJ 07102
e-mail: maciej.skotak@njit.edu

E. Alay
Department of Biomedical Engineering,
Center for Injury Biomechanics, Materials
and Medicine,
New Jersey Institute of Technology,
University Heights,
Newark, NJ 07102
e-mail: ea79@njit.edu

G. Unnikrishnan
Department of Defense,
Biotechnology High Performance Computing
Software Applications Institute,
Telemedicine and Advanced Technology
Research Center,
U.S. Army Medical Research and Materiel
Command,
504 Scott Street,
Fort Detrick, MD 21702
e-mail: gunnikrishnan@bhsai.org

H. Mao
Department of Defense,
Biotechnology High Performance Computing
Software Applications Institute,
Telemedicine and Advanced Technology
Research Center,
U.S. Army Medical Research and Materiel
Command,
504 Scott Street,
Fort Detrick, MD 21702
e-mail: hmao@bhsai.org

X. Duan
Department of Defense,
Biotechnology High Performance Computing
Software Applications Institute,
Telemedicine and Advanced Technology
Research Center,
U.S. Army Medical Research and Materiel
Command,
504 Scott Street,
Fort Detrick, MD 21702
e-mail: xduan@bhsai.org

Assessment of the Effectiveness of Combat Eyewear Protection Against Blast Overpressure

It is unclear whether combat eyewear used by U. S. Service members is protective against blast overpressures (BOPs) caused by explosive devices. Here, we investigated the mechanisms by which BOP bypasses eyewear and increases eye surface pressure. We performed experiments and developed three-dimensional (3D) finite element (FE) models of a head form (HF) equipped with an advanced combat helmet (ACH) and with no eyewear, spectacles, or goggles in a shock tube at three BOPs and five head orientations relative to the blast wave. Overall, we observed good agreement between experimental and computational results, with average discrepancies in impulse and peak-pressure values of less than 15% over 90 comparisons. In the absence of eyewear and depending on the head orientation, we identified three mechanisms that contributed to pressure loading on the eyes. Eyewear was most effective at 0 deg orientation, with pressure attenuation ranging from 50 (spectacles) to 80% (goggles) of the peak pressures observed in the no-eyewear configuration. Spectacles and goggles were considerably less effective when we rotated the HF in the counter-clockwise direction around the superior-inferior axis of the head. Surprisingly, at certain orientations, spectacles yielded higher maximum pressures (80%) and goggles yielded larger impulses (150%) than those observed without eyewear. The findings from this study will aid in the design of eyewear that provides better protection against BOP. [DOI: 10.1115/1.4039823]

[1]Corresponding author.
Manuscript received August 7, 2017; final manuscript received March 19, 2018; published online April 19, 2018. Assoc. Editor: Barclay Morrison.

S. T. Williams
Visual Protection and Performance Division,
U.S. Army Aeromedical Research Laboratory,
Bldg. 6901, Farrel Road,
Fort Rucker, AL 36362
e-mail: steven.t.williams26.ctr@mail.mil

T. H. Harding
Visual Protection and Performance Division,
U.S. Army Aeromedical Research Laboratory,
Bldg. 6901, Farrel Road,
Fort Rucker, AL 36362
e-mail: thomas.h.harding.civ@mail.mil

N. Chandra
Department of Biomedical Engineering,
Center for Injury Biomechanics, Materials and Medicine,
New Jersey Institute of Technology,
University Heights,
Newark, NJ 07102
e-mail: namas.chandra@njit.edu

J. Reifman[1]
Department of Defense,
Biotechnology High Performance Computing Software Applications Institute,
Telemedicine and Advanced Technology Research Center,
U.S. Army Medical Research and Materiel Command,
504 Scott Street,
Fort Detrick, MD 21702
e-mail: jaques.reifman.civ@mail.mil

Introduction

Exposure to explosive devices has been associated with 80% of eye injuries observed in United States (U.S.) Service members deployed to the recent conflicts in Iraq and Afghanistan [1]. This includes members who wore eye protection (24%; 34% of whom wore spectacles, 22% goggles, and the rest wore non-U.S. Department of Defense issued eyewear), members who did not (34%), and those whose use of eyewear protection is not known [1]. The shock wave, and the subsequent blast wind, resulting from such high-energy explosive devices can lead to different types of eye injuries. These include those potentially caused by the direct interaction of the blast wave itself with the eyes (i.e., primary blast injury) as well as injuries caused by the contact of objects with the eyes, including both blunt force trauma and penetrating trauma (e.g., from impinging shrapnel) [2]. Therefore, since 2005, Service members have been required to use protective eyewear, such as spectacles and goggles, during training and deployment [3]. Puzzlingly, while this requirement reduced the number of penetrating eye injuries, proving to be effective against shrapnel, no such relationship was observed for nonpenetrating injuries, i.e., closed-eye injuries [4].

One possible explanation is that military-issued eyewear is not effective against blast waves. However, to date, there is no consensus on whether a blast wave alone can cause eye injury [5]. This is because in a battlefield environment, Warfighters can be simultaneously exposed to a blast wave, blunt force trauma, and shrapnel, making it nearly impossible to isolate a primary blast injury from the other types of eye injuries. In contrast, studies using different rodent animal models have shown that exposure to a blast wave alone can cause eye injury. For example, incident pressures above 120 kPa can cause corneal edema and photoreceptor cell loss in mice [6], a decrease in retinal ganglion cell response in mice [7], and damage to cells of the optic nerves in rats [8]. These results suggest that a blast wave can potentially cause eye injury in humans as well. Indeed, recent finite element (FE) studies have investigated the potential causes of primary-blast-induced eye injury, suggesting different mechanisms of injury without providing, difficult-to-obtain, supporting experimental evidence [9,10].

Bailoor and colleagues investigated the effectiveness of eyewear in reducing the blast-induced pressure, the so-called blast overpressure (BOP), on the eyes [11]. They performed three-dimensional (3D) FE simulations using models of a human head equipped with spectacles and goggles, and used the mass of trinitrotoluene and stand-off distance as input conditions in their model to simulate the incident BOP. They reported that both spectacles and goggles offer protection, with goggles providing greater protection than spectacles at BOPs of 53 and 216 kPa. However, they used a mechanically rigid model for representing the goggles, which may eliminate loading on the eyes due to deflection of the goggles, and did not incorporate the soft padding of the goggles in the model, creating a gap between the goggles and the face, which can lead to incorrect predictions of the pressure on the eyes. Moreover, this study only investigated eyewear effectiveness with the head model directly facing the blast wave, and only reported experimental results for the maximum pressure on the eyes, with no comprehensive comparison between experimental data and simulations. In addition, none of these studies revealed potential

correlations between blast wave parameters (e.g., peak overpressure, impulse, or positive time duration) and eye injury.

The objective of this work was to assess the effectiveness of combat eyewear against BOP by performing experiments and 3D FE simulations. In particular, using the FE model, we sought to characterize the mechanisms by which BOP bypasses eyewear and loads the surface of the eyes at different head orientations relative to the oncoming blast wave. In total, we investigated 45 conditions, including a head form (HF) with no eyewear, spectacles, or goggles, five different head orientations relative to the oncoming blast wave, and three BOPs.

Materials and Methods

Shock Tube Experiments. We used a compressed-gas shock tube located at the New Jersey Institute of Technology. The shock tube had a cylindrical driver section (197 mm in inner diameter) that transitioned to a square-driven section with a cross-sectional length of 711 mm, which housed the test section (Fig. 1(*a*)). The driver and driven sections were 438- and 6871-mm long, respectively, and were separated by several frangible Mylar membranes. We pumped helium into the driver section until the membranes ruptured and generated a Friedlander-type blast wave [12]. We measured the static pressure-time profile of the blast wave at a point 2,946 mm from the membranes using a pressure sensor (model 134A24; PCB Piezotronics, Depew, NY) with its sensing surface parallel to the flow of the blast wave. For data acquisition, we used a custom LabVIEW code running on a National Instruments PXI-6133 S Series multifunction data acquisition modules and PXIe-1082 PCI Express chassis. We recorded the data at a sampling frequency of 1.0 MHz.

We developed a human head form using a polyurethane resin (BC 8007-2; Prospector, Overland Park, KS). The head height (the distance between the tragion and the top of the head) conformed to that of the 50th percentile male based on the U.S. Army anthropometric survey [13]. The head form had two hollow shafts, one at the left cornea and the other at the right cornea, which were equipped with a pressure sensor (model 113B26; PCB Piezotronics, Depew, NY) to measure the surface pressure on each eye. We fastened the head form rigidly in the driven section at a distance of 3,310 mm from the membranes. We used a large advanced combat helmet (ACH) for head protection, and separately tested the Revision Sawfly spectacles (Revision Military, Essex Junction, VT) and the Arena Flakjak goggles (Arena Tactical, Orange, CA) (Fig. 1(*a*)). We chose Revision Sawfly spectacles and Arena Flakjak goggles because, when we conducted this study, they were included in the authorized protective eyewear list. We placed the eyewear on the head form and marked reference points on the head form. Then, before each test in the shock tube, we adjusted the eyewear to align with these reference points.

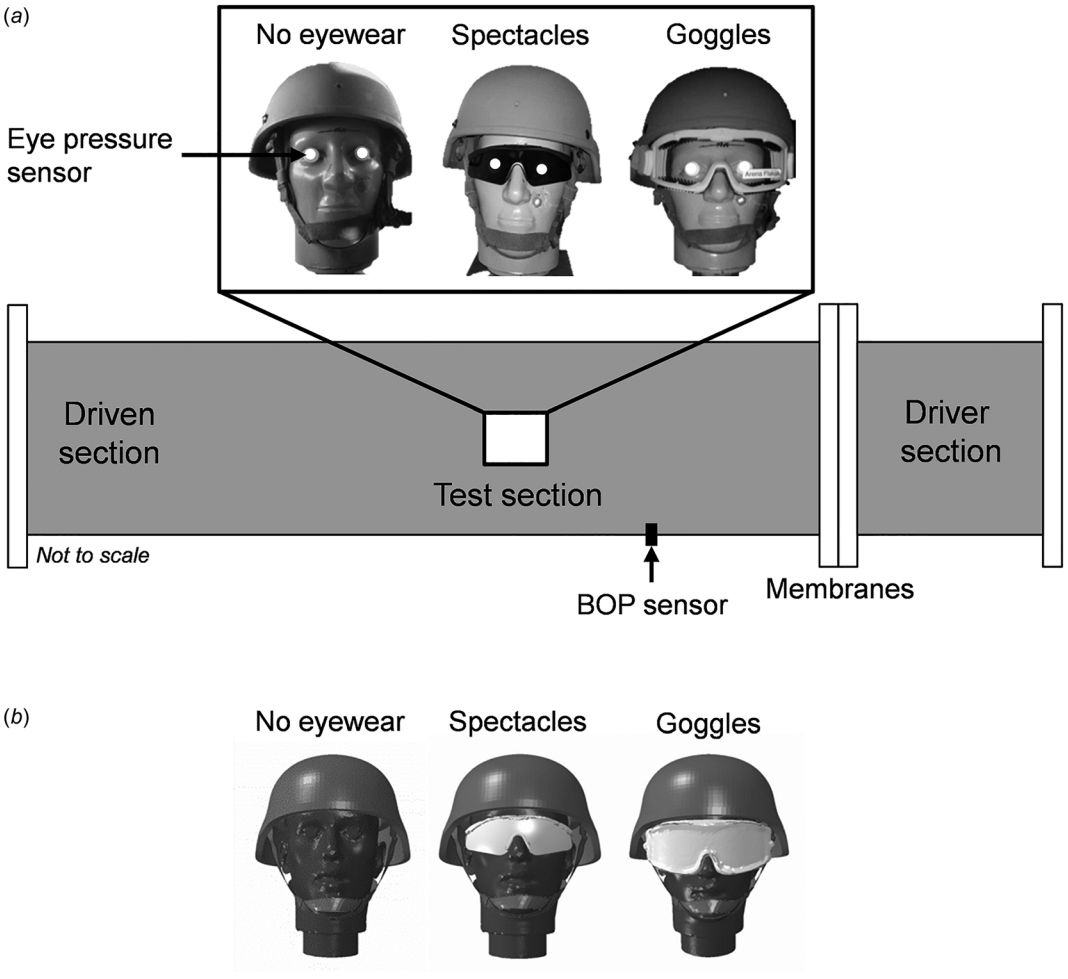

Fig. 1 (*a*) Schematic representation of a 711-mm square cross-sectional shock tube, indicating the driver section, driven section, and test section. We used a BOP sensor to measure the pressure of the oncoming blast wave in the driven section. We equipped the HF used in the experiment with two pressure sensors, one on each eye, outfitted the HF with an ACH, and assessed two eyewear protective equipment, the revision Sawfly spectacles and the Arena Flakjak goggles. (*b*) FE model of the head equipped with ACH for no eyewear, spectacles, and goggles.

Table 1 Material properties for spectacles and goggles

Eyewear	Component	Material	Density (kgm^{-3})	Young's modulus (MPa)	Poisson's ratio	References
Spectacles	Lens and frame	Polycarbonate	1220	2400	0.37	[15]
Goggles	Frame	Neoprene	1300	5	0.45	[15]
	Lens	Polycarbonate	1220	2400	0.37	[15]
	Foam	Soft foam	136	1	0.21	[14,16,17]

Finite Element Model. Similar to the previous studies that have modeled shock tubes, our FE model represented a portion of the driven section of the experimental shock tube [14]. The modeled portion was 1300-mm long and had a square cross-sectional length of 711 mm. We meshed the geometry with eight-noded hexahedral Eulerian elements using a biased meshing technique in ABAQUS (Dassault Systèmes, Vélizy-Villacoublay, France). With this technique, we assigned finer elements near the eyes of the head form and coarser elements elsewhere in the shock tube FE model. Finally, we assigned an ideal gas material property with an adiabatic constant of 1.4, a density of 1.2 kg·m^{-3}, and a temperature of 300 K for the atmospheric air within the shock tube FE model.

To represent the head form, ACH, spectacles, and goggles in our 3D FE model, we digitized them with a Creaform HandyScan 300 scanner (Creaform, Costa Mesa, CA) to create surface mesh models. Then, we imported these models into HyperMesh 12.0 (Altair, Inc., Troy, MI) (Fig. 1(*b*)). Next, we converted the head form and ACH surface meshes to discretely rigid shell elements (not deformable), and converted the surface mesh of the spectacles and goggles to a ten-node quadratic tetrahedral mesh (deformable). Finally, we assigned homogenous, isotropic elastic material properties to both spectacles and goggles (Table 1) [14–17].

We applied the BOPs measured in front of the head (Fig. 1(*a*)) during the experiments as an inlet boundary condition to the shock tube FE model. For the remaining surfaces of the model, we constrained the displacement in the direction perpendicular to each surface. The spectacles and goggles used in the model were not constrained; however, we constrained the head form and ACH along all degrees-of-freedom. Finally, as described by Ganpule and colleagues, we used the coupled Eulerian–Lagrangian method in ABAQUS to simulate blast-wave propagation [14].

Test Conditions and Mesh Convergence. We outfitted the head form with the ACH without eyewear, and performed shock-wave exposure experiments and computer simulations at BOPs of 70, 140, and 210 kPa, with the head facing the oncoming blast wave (0 deg orientation). Next, we rotated the head counterclockwise by 45, 90, 135, and 180 deg to study the effect of head orientation on eye surface pressure (Fig. 2(*a*)). Then, we separately equipped the head with spectacles or goggles and repeated the studies for the same BOPs and head orientations. Overall, we performed 45 simulations and 135 experiments (3 per condition), measuring the pressure on the left and right eyes (REs). Finally, to assess the accuracy of the simulations, we compared the pressure-time profiles, their integrated values (i.e., the impulse), and the maximum pressure between the experiments and simulations.

We performed mesh convergence studies for the shock tube elements using a 70 kPa BOP loading for each eyewear condition and determined 1.5 mm as an adequate edge length for the elements. With the biased meshing technique, we assigned 1.5-mm edge-length elements near the eyes and coarser elements elsewhere, which helped us reduce the total number of elements used for meshing the shock tube FE model from 194.7 to 4.1 million without affecting the accuracy of the results.

Results

Incident Blast Overpressures. Figure 2(*b*) shows the experimentally measured pressure-time profiles of incident blast waves for 70, 140, and 210 kPa. Each pressure-time profile had a Friedlander-type waveform, with a nearly instantaneous rise to the peak overpressure followed by an exponential-like decay.

Validation of Finite Element Models. To validate our FE model, we compared the experimentally obtained and simulated values of peak pressure on the surface of the eyes (Fig. 3 and Table 2). We observed good overall agreement between the simulations (bars) and the experiments (markers), with a mean error of 15% [standard deviation (SD) = 12%] over 90 comparisons on both eyes. We observed no systematic reason for such differences. Furthermore, we analyzed Pearson's correlation between the simulated and experimental values of maximum pressure, which yielded R^2 values of 0.98 and 0.95 for the left and right eyes, respectively. By comparing the experimental and simulated pressure-time profiles for all BOPs and orientations, we observed that our model also captured the essential features of the

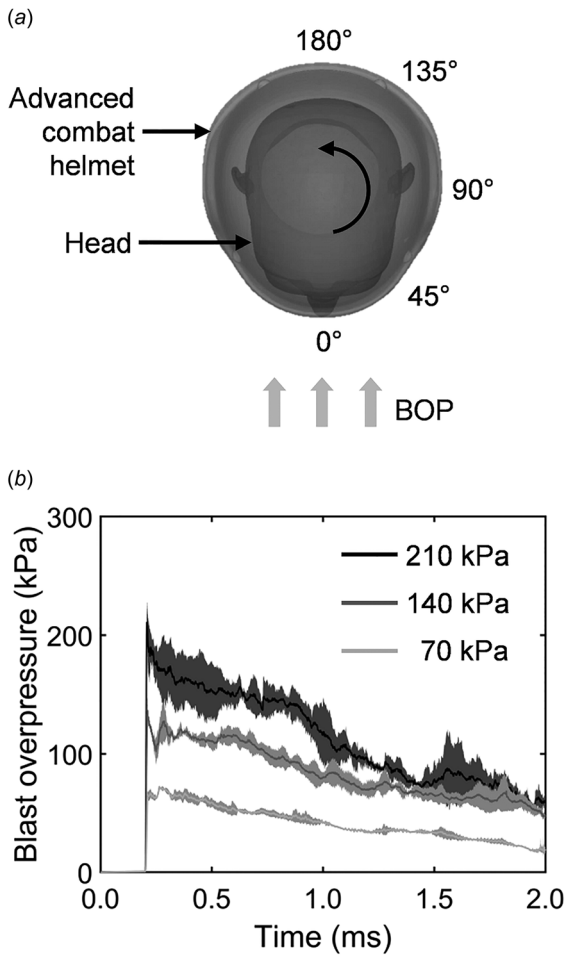

Fig. 2 (*a*) We investigated the effects of orientation by performing experiments and simulations at five orientations 0 (head on), 45, 90, 135, and 180 deg with and without eyewear and (*b*) experimentally measured pressure-time profiles ($N = 3$) for incident BOPs of 70, 140, and 210 kPa (line and shaded region; mean ± one standard deviation)

experimental profiles. Figures 4 and 5 compare the experimental and simulated profiles for the left eye (LE) and the right eye, respectively, at a BOP of 210 kPa. The figures show that the simulated profiles captured key features of the experiment, such as the multiple peaks observed on the right eye for 90 and 135 deg orientations. In addition, we compared the impulse (the area under the pressure-time profile) between experiments and simulations. This also yielded good overall agreement with a mean error of 13% (SD = 9%) over 90 comparisons on both eyes (Table 3). We also analyzed Pearson's correlation between the simulated and experimental values of impulse, which yielded R^2 values of 0.94 and 0.91 for the left and right eyes, respectively.

No-Eyewear Condition

Maximum Eye Surface Pressure. We investigated the interactions between the blast wave and eyes by varying the BOP and the angle of blast exposure (where 0 deg indicated the condition when the head directly faced the oncoming blast wave), and then measuring the maximum eye surface pressures. From our simulations, without eyewear at 0 deg, for both eyes, a BOP of 70 kPa led to a maximum pressure of 216.33 kPa, while a BOP of 140 kPa resulted in a maximum pressure of 465.95 kPa. Hence, the maximum pressure increased by approximately threefold relative to the incident BOP (Fig. 3 and Table 2). Interestingly, a BOP of 210 kPa resulted in an average maximum eye surface pressure for both eyes of 1114.95 kPa, a fivefold increase relative to the incident BOP.

Pressure-Time Profiles. For no eyewear at 0 deg and 210 kPa, the experimental and simulated pressures on the eyes rose to their peak values, and then decayed exponentially on both eyes (Figs. 4 and 5, top left). Interestingly, the pressure on the left eye, at 90 and 135 deg orientations, after an initial rise, decayed exponentially after an initial rise and then began to increase again at ~0.5 ms (Fig. 4). On the right eye, we observed two distinct peaks in the pressure-time profiles at 90 and 135 deg (Fig. 5). At 180 deg orientation, the pressure-time profiles for both eyes showed delayed peaks, which were considerably higher than those at 90 and 135 deg, followed by an exponential decay.

Impulse. For no eyewear at each BOP, both experiments and simulations showed that the impulse on the left eye decreased monotonically when we rotated the head in the counter-clockwise direction from 0 to 90 deg (Table 3). However, it increased when we rotated the head from 90 to 180 deg. Interestingly, at 135 deg and all BOPs, the impulse on the left eye was higher than that on the right eye.

Effect of Spectacles

Maximum Eye Surface Pressure. From simulations, with the spectacles at a BOP of 70 kPa and 0 deg orientation, we observed that the maximum pressure decreased by an average of ~50% on both eyes (Fig. 3, top). Furthermore, for BOPs of 140 and 210 kPa, the percentage reduction in eye surface pressures increased to ~60 and ~75%, respectively (Fig. 3, middle and bottom). Interestingly, beyond 45 deg for all BOP intensities, spectacles offered little benefit, and in some cases, resulted in higher pressures than those for no eyewear (e.g., 70 kPa at 90 deg, 140 kPa at 180 deg, and 210 kPa at 90 deg).

Pressure-Time Profiles. From both experiments and simulations, with the spectacles for a BOP of 210 kPa at 90 and 135 deg orientations, similar to the no-eyewear condition, the pressure on the left eye decayed exponentially followed by a pressure rise at ~1.0 and 0.5 ms, respectively (Fig. 4).

Effect of Goggles

Maximum Eye Surface Pressure. From both experiments and simulations, with the goggles at 0 deg, the maximum pressure decreased by an average of ~80% on both eyes for all BOPs (Fig. 3). Likewise, at 45 and 90 deg, we observed a decrease in left and right eye surface pressures relative to the no-eyewear condition. Interestingly, at 135 deg orientation, the maximum pressure on the left eye was higher with the goggles than it was in the no-eyewear condition at all three BOPs.

Pressure-Time Profiles. From both experiments and simulations, the use of goggles resulted in a markedly longer rise time to maximum pressure than the no-eyewear and spectacles conditions for all orientations and BOPs (Figs. 4 and 5).

Impulse. From our simulations, with the goggles at 90 deg orientation and 70 kPa BOP, we observed a ~25% increase in the impulse on the left eye, when compared to the no-eyewear condition (Table 3). Similarly, at BOPs of 140 and 210 kPa, the impulse on the left eye increased by ~65 and ~180%, respectively. We observed a similar trend in the impulse from our experimental results.

Discussion

We investigated the effectiveness of combat eyewear against primary blast exposure and determined the mechanisms by which blast waves load the surface of the eyes with and without eyewear protection. Specifically, we characterized the effectiveness of the eyewear using physical and simulated models of a head form with and without eyewear to experimentally measure and computationally determine the temporal evolution of pressure on the eyes, their integrated values (i.e., the impulse), and the maximum eye surface pressures caused by oncoming blast waves of 70, 140, and 210 kPa at five orientations (from 0 to 180 deg at 45 deg increments). We chose these pressures because the previous animal model studies have shown that blast waves can cause eye injury when the BOP exceeds 120 kPa [6–8]. Overall, we observed good agreement between experimental and computational results, with average impulse and peak-pressure discrepancies of less than 15% over 90 comparisons. To determine the mechanisms of blast loading to the surface of the eyes, we evaluated the development of pressure patterns in our FE simulations.

Our simulations suggest that in the absence of eyewear, three mechanisms contribute to pressure loading on the eyes: (1) direct interaction of the BOP with the eyes, (2) reflection of the BOP from facial features, such as the nose, cheeks, and forehead, and (3) a pressure surge (PS) around the head due to the combination of diffracted pressures (Fig. 3). At 0 deg orientation, the maximum pressure on both eyes was approximately threefold higher than the applied BOPs of 70 and 140 kPa. Our simulations suggest that this increase is due to a combination of two of these mechanisms. First, when the BOP directly interacted with the eye surface normally, the incident pressure was transformed into reflected pressure. This reflected pressure has been estimated to be between 2 and 8 times the incident BOP [18]. Second, our simulations demonstrated that the reflected pressures from the nose, forehead, and cheek funneled toward the eyes, which then combined with and amplified the pressure on the eyes (in front of the cornea). Similarly, using a FE model of a human head, Bhardwaj et al. also predicted that reflections from facial features influence the pressure loading on the eyes [9]. Although the mechanisms of loading did not change with an increase in the BOP, we observed a fivefold increase in the maximum eye surface pressures at 210 kPa. This increase was due to the nonlinear increase in the reflected pressure when we increased the BOP [18].

In contrast to the pressure-time profile at the 0 deg orientation, the profiles for the right eye at orientations of 90 and 135 deg with no eyewear had two peaks followed by an exponential decay (Fig. 5, left column). The first peak was due to the direct interaction of the BOP with the eye. Subsequently, the pressure reflected off the nose reloaded the eye to form the second peak. In this case, only two mechanisms—the direct interaction of the BOP with the eye and the reflection of the pressure wave from the nose—

contributed to the total pressure load on the right eye. Figure 6(*a*) shows the simulated temporal pressure evolution on the right eye at the 90 deg orientation. The direct interaction occurred at 0.27 ms, whereas the reloading by the pressure reflected off the nose occurred at 0.36 ms.

For the left eye, at 90 and 135 deg with no eyewear, the pressure first declined after reaching an initial peak, and then increased again, albeit at different rates and to different levels relative to the first peak (Fig. 4, left column). Our simulations showed that this secondary increase was due to the pressure surge originating from a combination of diffracted pressures around the head, which moved toward and reloaded the left eye. Figure 6(*b*) illustrates this process at 135 deg, where the surge formed around the head at 0.58 ms and the subsequent loading on the left eye occurred at 0.75 ms. Because for this orientation the left eye was closer to the surge than the right eye and because at this time the pressure from the direct interaction was still unloading the eyes, unexpectedly, the left eye experienced higher pressures and larger impulses than the right eye for all BOPs.

Finally, at 180 deg with no eyewear, our simulations showed that the blast waves diffracted by the helmet engulfed the head and directly loaded the eyes. Subsequently, the pressure reflected off the nose reloaded both eyes and, at the same time, the waves diffracted from both sides of the head combined in front of the head and generated a pressure surge that loaded the eyes. Therefore, at this orientation, all three mechanisms contributed to the pressure loading on the eyes.

With spectacles at 0 deg, the maximum eye surface pressures decreased by ~50% relative to the no-eyewear condition at a BOP of 70 kPa (Fig. 3, top row). Our simulations suggest that this reduction occurred because the spectacles prevented the blast wave from directly loading the eyes. However, the pressure reflected off the cheek entered through the gap between the spectacles and the face, and then loaded the eyes indirectly.

Table 2 Peak eye surface pressure from experiments ($N = 3$) and simulations on the left and REs at BOPs of 70, 140, and 210 kPa for three eyewear conditions and five head orientations relative to the incident BOP

			Peak eye surface pressure (kPa)			
			Left eye		Right eye	
Blast overpressure (kPa)	Eyewear type	Counter-clockwise orientation (Deg)	Experiment ($N = 3$) [Mean (SD*)]	Simulation	Experiment ($N = 3$) [Mean (SD*)]	Simulation
70	No eyewear	0	218.05 (6.05)	218.11	194.64 (4.44)	214.55
		45	126.93 (5.78)	141.60	192.14 (16.29)	195.30
		90	52.82 (1.12)	57.03	102.93 (0.95)	99.87
		135	62.51 (2.94)	58.11	53.29 (1.00)	64.65
		180	70.68 (2.52)	55.11	63.51 (2.39)	55.99
	Spectacles	0	140.37 (11.00)	99.93	134.73 (21.98)	114.22
		45	124.60 (15.52)	126.06	144.38 (15.34)	139.81
		90	66.47 (5.27)	65.92	114.55 (3.49)	106.35
		135	59.48 (1.84)	52.84	86.93 (0.69)	89.85
		180	70.77 (4.17)	72.68	66.55 (1.61)	72.23
	Goggles	0	41.44 (1.77)	42.07	40.70 (5.97)	39.28
		45	41.69 (0.80)	40.30	38.55 (0.87)	30.18
		90	40.81 (0.60)	36.03	35.29 (1.48)	34.37
		135	67.27 (2.83)	60.68	47.76 (0.83)	37.40
		180	64.97 (2.61)	47.07	48.05 (2.63)	56.64
140	No eyewear	0	532.82 (53.56)	459.35	537.59 (38.66)	472.55
		45	297.79 (2.84)	259.09	492.25 (8.31)	386.31
		90	121.39 (4.72)	140.92	179.12 (10.25)	239.17
		135	94.90 (0.51)	95.12	77.47 (5.36)	110.47
		180	138.46 (8.78)	116.94	134.70 (6.46)	109.24
	Spectacles	0	241.72 (24.59)	175.40	234.26 (10.42)	215.18
		45	207.02 (17.06)	242.46	323.57 (34.38)	361.80
		90	127.10 (11.52)	141.46	261.54 (30.99)	240.35
		135	116.86 (10.72)	96.12	159.28 (4.88)	109.61
		180	132.33 (7.12)	157.93	126.53 (9.37)	127.20
	Goggles	0	108.72 (14.39)	87.33	96.73 (16.04)	82.66
		45	96.64 (17.07)	72.33	95.14 (12.97)	62.86
		90	78.91 (9.88)	74.66	82.79 (3.37)	68.07
		135	124.39 (5.47)	104.95	81.98 (3.43)	74.58
		180	101.68 (6.14)	92.69	96.01 (4.54)	111.35
210	No eyewear	0	1064.53 (121.88)	1064.90	1049.69 (122.09)	1165.03
		45	403.90 (61.48)	384.97	780.31 (132.14)	678.68
		90	136.12 (18.20)	117.31	179.57 (29.74)	207.62
		135	103.89 (1.65)	92.44	99.20 (6.96)	114.90
		180	201.57 (15.71)	210.13	172.28 (16.79)	178.41
	Spectacles	0	322.77 (35.88)	239.20	342.77 (62.52)	252.26
		45	283.36 (12.86)	254.16	525.09 (117.85)	391.64
		90	186.78 (16.07)	173.11	412.55 (116.96)	307.41
		135	139.85 (14.95)	92.34	176.39 (9.46)	211.89
		180	182.83 (6.65)	195.76	166.38 (5.72)	144.06
	Goggles	0	171.06 (21.95)	187.45	175.63 (15.33)	184.56
		45	127.85 (7.77)	112.93	149.74 (3.44)	146.97
		90	84.07 (2.07)	99.11	120.64 (8.38)	102.36
		135	148.72 (6.60)	108.76	102.54 (6.26)	78.17
		180	122.42 (5.56)	108.89	142.90 (10.17)	123.76

Subsequently, the pressure rebounded off the brow ridges and started to travel back-and-forth in the pocket between the face and the inner wall of the spectacles, which further increased the eye surface pressure. These findings are consistent with those reported by Bailoor et al., who used a FE model of a human head equipped with spectacles [11]. Interestingly, with the use of spectacles, an increase in the BOP resulted in an increase in the percentage reduction in the eye surface pressures. This is because the spectacles prevented the formation of reflected pressure, which increased nonlinearly with an increase in the BOP for the no-eyewear condition.

For the right eye, at 90 and 135 deg, the gap between the face and the spectacles was directly exposed to the blast wave. Under this condition, our simulations showed that the pressure wave entered through the gap and loaded the right eye. Then, the wave reflected off the nose reloaded the eye, generating a second peak (Fig. 5, middle column). Next, owing to the back-and-forth interaction, the pressure further increased within the pocket. This surge in pressure was responsible for the third peak observed in the simulated pressure-time profile. In contrast to the no-eyewear condition, which showed only two peaks (Fig. 5, left column), the spectacles caused this rise in pressure by preventing the pressure reflected off the nose to expand and dissipate. As a consequence, the use of spectacles was not beneficial at these orientations. For the left eye, at 90 and 135 deg, as seen in the no-eyewear condition, the pressure first decayed after reaching an initial peak, and then increased again (Fig. 4, middle column). This increase was due to the pressure surge from the diffracted pressures that entered through the gap between the spectacles and the face and reloaded the eye. Although the eye surface pressure was higher with spectacles compared to the no-eyewear condition at the 90 deg orientation, it is important to note that the peak pressures reached were still lower than those at the 0 and 45 deg orientations.

At 180 deg, the BOP entered through the gap between the spectacles and the face on the side of the spectacles (near the temples) and loaded both eyes. Subsequently, the pressure loading on the eyes increased in intensity within the pocket formed by the inner wall of the spectacles with the nose and the face.

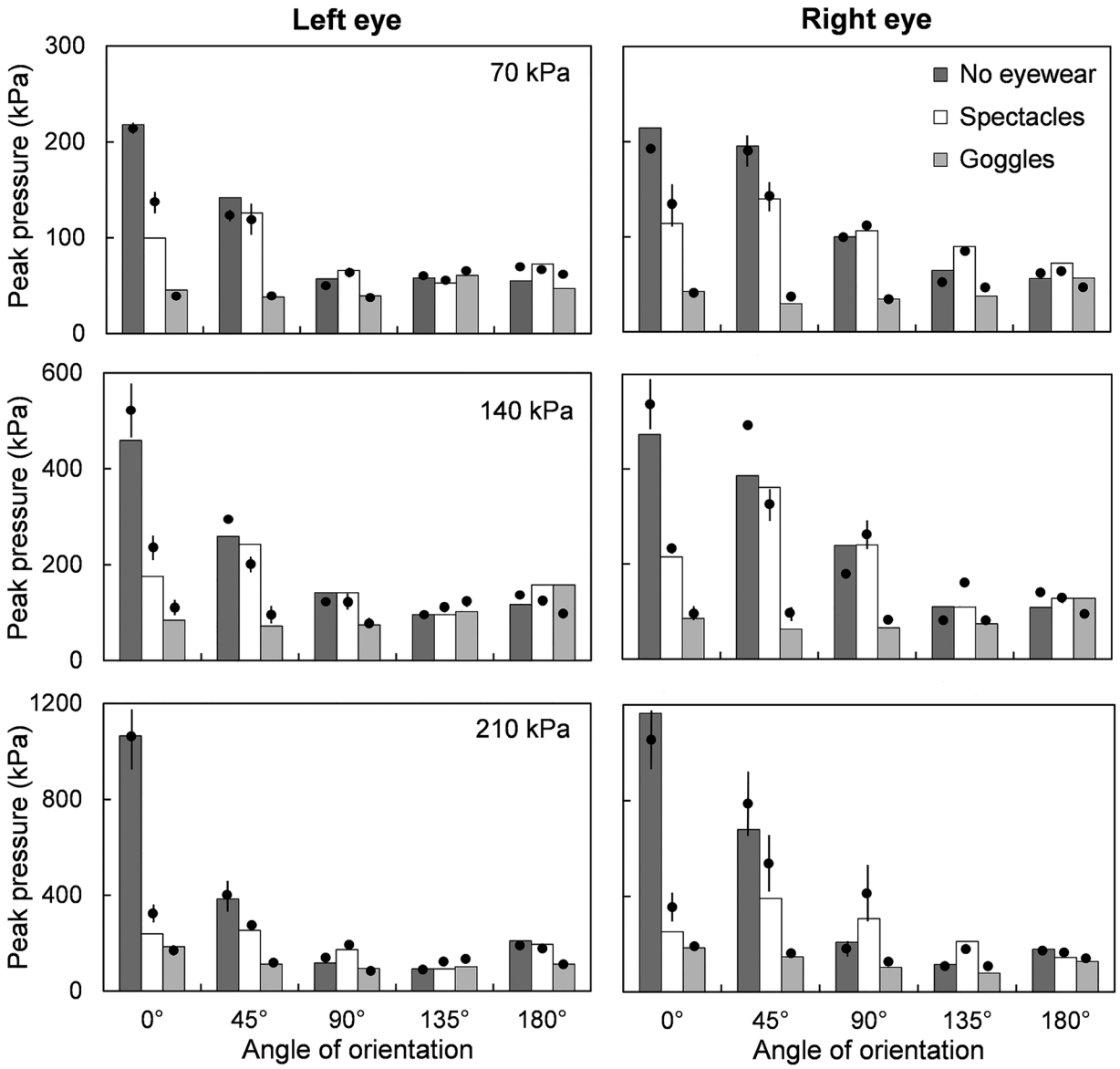

Fig. 3 Maximum average pressure from experiments (markers and vertical lines; mean ± one standard deviation) ($N = 3$) and simulations (bars) on the left and right eyes at BOPs of 70, 140, and 210 kPa for three eyewear conditions and five head orientations relative to the incident BOP

Simultaneously, the waves diffracted by the helmet combined in front of the head and formed a pressure surge, which the spectacles prevented from directly interacting with the eyes. However, it entered through the gap between the spectacles and the face, and loaded the eyes.

With goggles at 0 deg, the maximum eye surface pressure decreased by ~80% relative to the no eyewear condition for all BOPs (Fig. 3). Our simulations showed that when the BOP impinged upon the goggles, the lens deflected inward and initiated a pressure wave within the goggles, which caused the primary loading on the eyes. Subsequently, the pressure wave underwent back-and-forth reflections in the pocket between the inner walls of the goggles and the face, which slowly increased the pressure on the eyes (Figs. 4 and 5, right column). Because the goggles fitted the face snugly, the pressure within the goggles dissipated more slowly than when using spectacles or in the no-eyewear condition. Consequently, the pressure on the eyes was sustained for a longer duration for all BOPs.

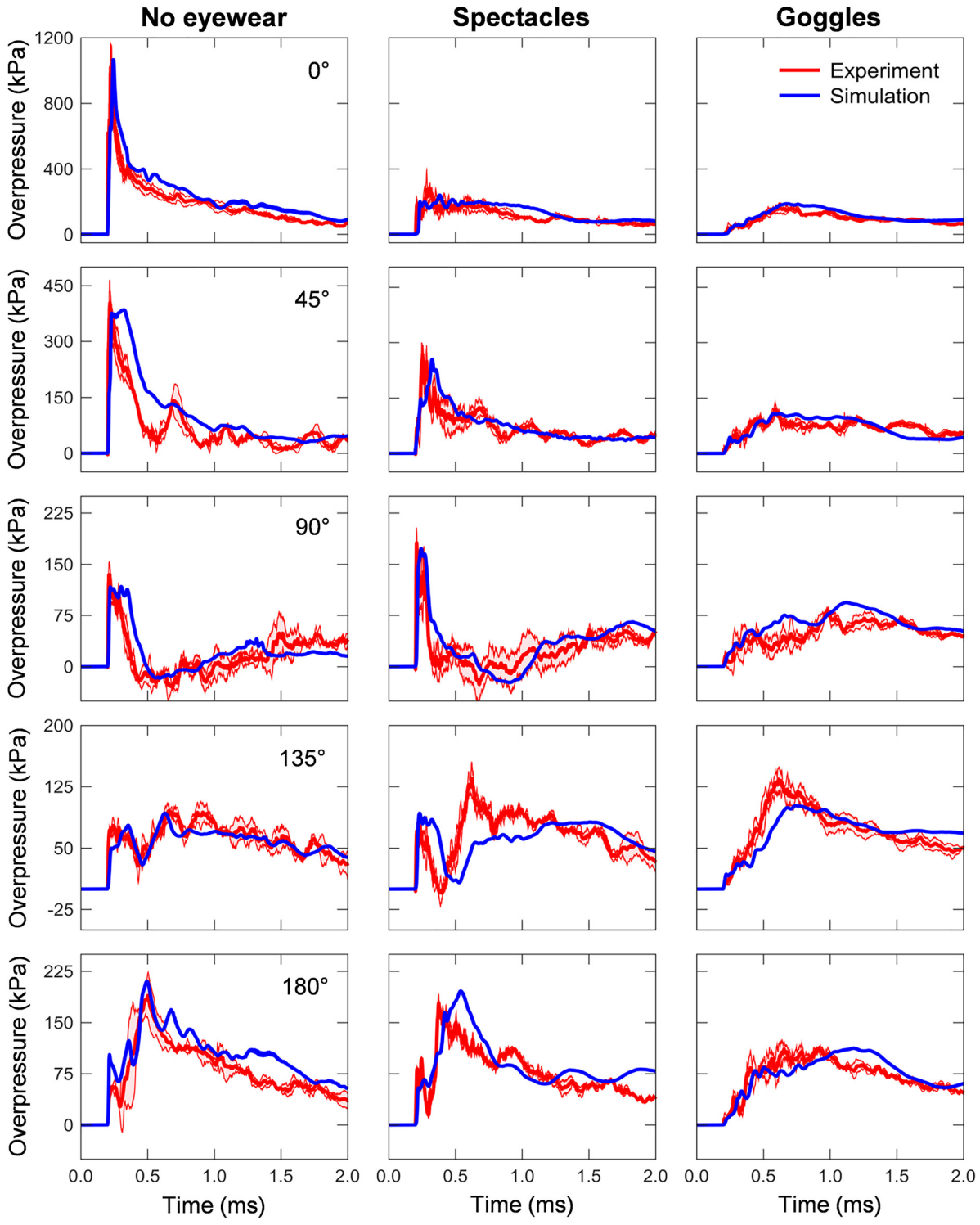

Fig. 4 Left eye surface pressure-time profile comparisons between experiments (red line (grey in B/W) and shaded region; mean ± standard deviation) ($N = 3$) and simulations (blue line (black in B/W)) at 210 kPa BOP for three eyewear conditions and five head orientations relative to the incident BOP

The maximum eye surface pressure with goggles was less than the no-eyewear condition for both eyes in almost all conditions (BOPs and orientations), with the exception of the left eye at 135 deg. At this orientation, the initial loading on the left eye occurred when the BOP impinged on the goggles. Then, the pressure surge from the combination of diffracted pressures also loaded the left side of the goggles, resulting in a higher left eye surface pressure relative to the no-eyewear condition for all BOPs (Figs. 3 and 4). At 180 deg, the goggles prevented the direct interaction of the combination of diffracted pressures with the eyes. Consequently, the pressures were lower relative to the no-eyewear condition for all BOPs.

Perhaps the most surprising finding of our work was that, in stark contrast to the maximum eye surface pressure, at a head orientation of 90 deg, the impulse on the left eye was substantially higher with goggles than without eyewear for all BOPs (Table 3), whereas the opposite was true for the maximum pressure (Fig. 3, left column). Our simulations showed that when the pressure

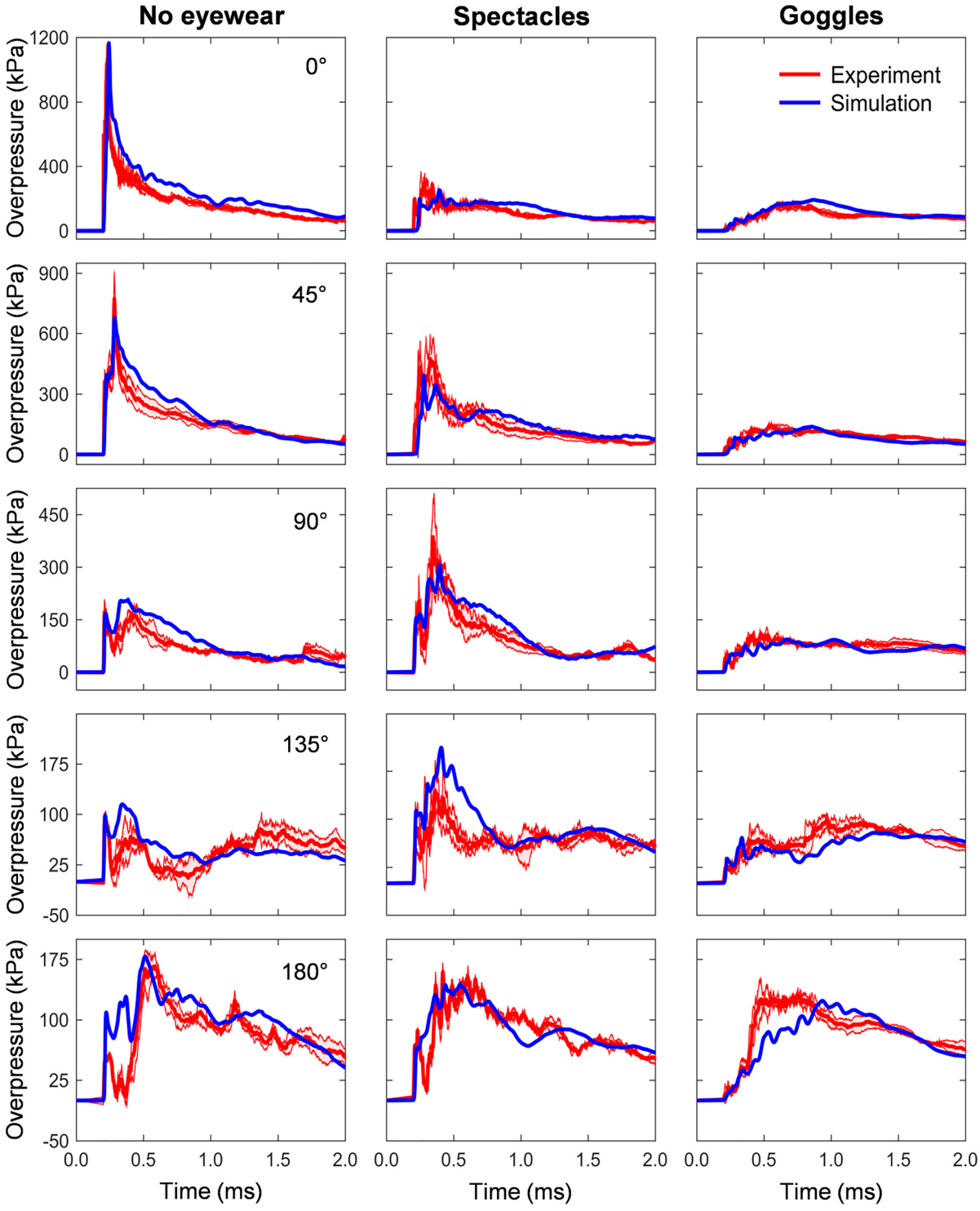

Fig. 5 Right eye surface pressure-time profile comparisons between experiments (red line (grey in B/W) and shaded region; mean ± standard deviation) ($N = 3$) and simulations (blue line (black in B/W)) at 210 kPa BOP for three eyewear conditions and five head orientations relative to the incident BOP

loading on the left eye from the direct interaction of the BOP with the goggles started to decay, the pressure loading from the combination of the diffracted pressures loaded and sustained the pressure on the eye (Fig. 4, right column, middle panel). Consequently, the pressure on the eye was prolonged, which resulted in a higher impulse than the no-eyewear condition despite the lower maximum pressure. Although these results suggest that goggles may not protect the eyes from BOP beyond the 90 deg orientation, they still perform better than spectacles in reducing surface pressure on the eyes and are protective against secondary blast injuries, which are the major cause of eye injuries in the field [2,4].

One limitation of our study was that we used an ideal Friedlander waveform, whereas in real-world conditions the loading pressure is more complex, because it is influenced by surrounding structures. Nevertheless, the use of such a waveform has become a standard practice when studying the effects of primary blast exposure mimicking an open-field environment. Second, in our FE model, we assumed the ACH, the head form, and the face, including the eyes, to be rigid materials. Although this might have resulted in slight overestimation of the eye surface pressures, we expect the findings discussed herein to remain valid despite such simplifications. Third, although our study design covered 45 distinct conditions, the realities of time and cost prevented us from studying certain configurations, such as head-form rotations upward and downward from the horizontal plane. Such a shortcoming notwithstanding, the benefit of a validated FE model is that it could reliably predict other configurations beyond those experimentally explored. Fourth, we mounted the head form rigidly to the shock tube, preventing its movement. This assumption does not realistically emulate loading conditions in the field because, in reality, relative motion between the body and the head can occur. To investigate the validity of this assumption, we performed an additional FE simulation where we changed the boundary condition and allowed the head form to move freely. When compared to the rigidly fixed head-form results, we observed no differences in the reflected pressure and surge effects, leading us to conclude that these responses occur within a few milliseconds

Table 3 Impulse from experiments ($N = 3$) and simulations on the left and REs at BOPs of 70, 140, and 210 kPa for three eyewear conditions and five head orientations relative to the incident BOP

			Left eye impulse (kPa·ms)		Right eye impulse (kPa·ms)	
Blast overpressure (kPa)	Eyewear type	Counter-clockwise orientation (Deg)	Experiment ($N = 3$) [Mean (SD*)]	Simulation	Experiment ($N = 3$) [Mean (SD*)]	Simulation
70	No eyewear	0	88.91 (1.96)	95.42	83.75 (1.55)	94.22
		45	60.83 (8.83)	68.48	80.02 (6.34)	94.36
		90	43.13 (1.34)	42.15	54.32 (0.54)	67.81
		135	69.23 (0.88)	58.19	38.06 (0.69)	56.16
		180	71.61 (1.93)	66.74	68.57 (0.79)	67.85
	Spectacles	0	79.80 (6.01)	103.64	69.11 (3.71)	97.86
		45	51.91 (0.20)	79.07	74.33 (2.08)	113.70
		90	50.38 (1.74)	53.24	63.63 (1.16)	82.67
		135	66.76 (2.55)	72.18	56.52 (7.29)	75.56
		180	75.55 (2.39)	68.91	70.92 (6.11)	68.17
	Goggles	0	63.34 (2.08)	57.91	52.55 (9.25)	57.79
		45	53.88 (2.40)	54.90	54.39 (1.81)	51.91
		90	57.25 (1.89)	53.92	52.80 (0.80)	47.58
		135	70.53 (1.59)	71.42	59.06 (0.98)	47.29
		180	69.63 (1.12)	69.72	66.11 (2.34)	71.86
140	No eyewear	0	202.91 (14.94)	225.69	197.29 (13.58)	229.70
		45	117.37 (3.90)	123.36	202.30 (4.32)	196.65
		90	51.10 (6.01)	66.82	124.50 (6.31)	186.12
		135	114.40 (0.73)	104.40	85.93 (12.20	91.38
		180	122.23 (5.01)	141.28	125.08 (7.77)	134.96
	Spectacles	0	129.46 (16.35)	176.15	134.75 (14.80)	141.55
		45	98.96 (5.32)	121.54	163.24 (7.97)	255.72
		90	62.29 (7.67)	56.46	133.73 (6.16)	138.22
		135	117.66 (2.39)	121.74	104.84 (5.78)	140.43
		180	125.79 (4.60)	149.21	122.53 (5.23)	143.40
	Goggles	0	119.77 (10.07)	123.01	119.90 (7.85)	122.26
		45	105.57 (8.78)	100.66	112.77 (7.55)	101.35
		90	91.39 (4.04)	111.60	102.11 (0.76)	114.85
		135	118.09 (5.08)	123.40	96.68 (10.07)	104.34
		180	107.30 (3.33)	124.48	103.55 (4.72)	133.64
210	No eyewear	0	359.71 (40.36)	456.04	339.35 (33.04)	453.97
		45	133.03 (6.13)	198.43	320.72 (36.60)	366.26
		90	39.44 (8.20)	45.88	132.03 (8.37)	112.28
		135	118.58 (10.17)	124.27	94.34 (13.86)	102.51
		180	156.70 (7.35)	202.20	164.89 (15.25)	192.52
	Spectacles	0	219.47 (20.50)	259.15	215.88 (12.25)	217.74
		45	138.90 (8.84)	157.16	272.55 (54.13)	293.15
		90	55.64 (18.16)	74.89	189.42 (31.85)	217.01
		135	128.31 (5.54)	123.33	139.07 (6.90)	169.42
		180	147.73 (4.97)	181.30	169.76 (3.79)	169.43
	Goggles	0	186.13 (14.98)	179.53	191.16 (12.55)	188.43
		45	135.37 (9.65)	141.83	180.07 (3.52)	170.13
		90	98.90 (2.73)	129.36	149.10 (8.49)	145.06
		135	150.21 (11.67)	135.61	137.98 (11.73)	117.38
		180	142.26 (3.14)	148.95	172.08 (4.21)	157.88

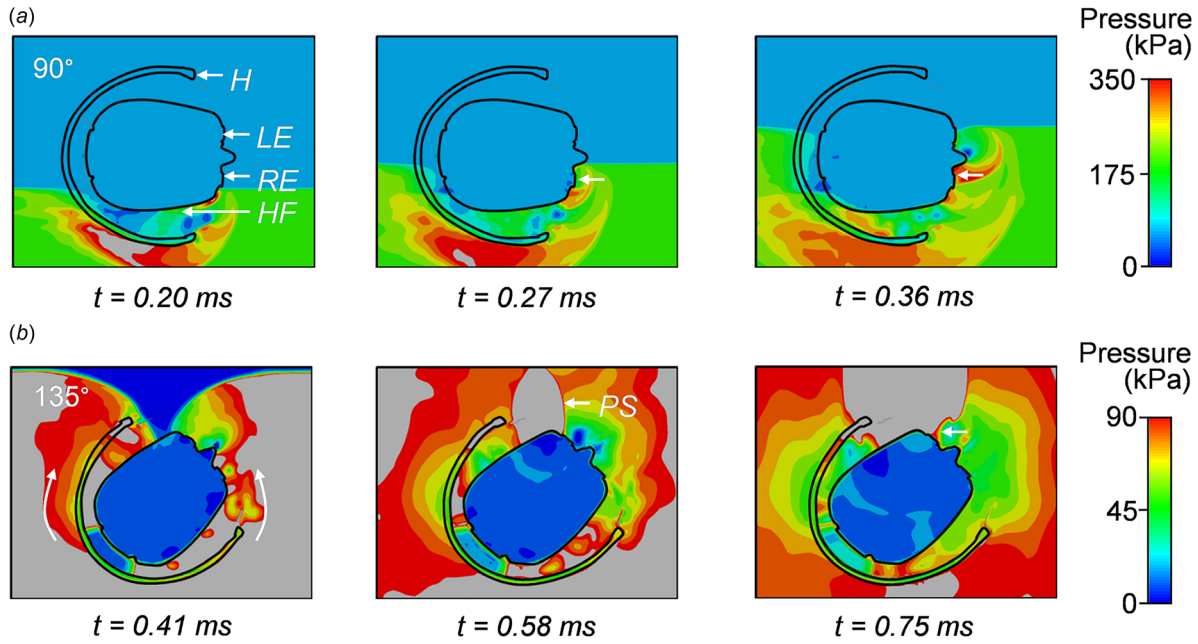

Fig. 6 Evolution of BOP on the LE and RE at the cross section of the HF and helmet (*H*) models seen from the top. (*a*) At 90 deg, we observed a BOP approaching the head at $t = 0.20$ ms, directly interacting (white arrow) with the RE at $t = 0.27$ ms, and reflecting off the nose and reloading the eye (white arrow) at $t = 0.36$ ms. (*b*) At 135 deg, we observed diffracted pressures engulfing the helmet and HF (white arrow) at $t = 0.41$ ms, followed by the formation of a PS from the combination of the diffracted pressures at $t = 0.58$ ms and the PS loading the LE (white arrow) at $t = 0.75$ ms.

after the blast wave interacts with the face during which the headform motion is negligible. Fifth, we modeled the eyewear using linear elastic material properties when most likely it is a viscoelastic material. Nevertheless, our comparison of the simulated peak eye surface pressures, pressure-time profiles, and impulse with 45 experiments suggests that this assumption has a small effect on the results. Finally, in the current form, our model cannot be used for predicting intraocular pressure or tissue strains. Therefore, we cannot make injury threshold predictions. Nonetheless, it revealed important insights on the mechanisms of BOP loading on the eyes at different orientations relative to the oncoming blast wave, with and without eyewear. Such knowledge is essential in developing a more detailed model, which may ultimately allow for such predictions in the future.

Conclusion

Our study revealed how a BOP with an ideal Friedlander waveform loads the eyes without and with eyewear (spectacles and goggles) on a rigid head form. We found that compared to Revision Sawfly spectacles, Arena Flakjak goggles offered better protection against such a BOP. However, the protective benefits depend on the shape and fit of the eyewear, as well as the size of the gap between the eyewear and the face. We also identified the mechanisms by which blast waves bypass these spectacles and goggles, and load the eyes at different head orientations relative to the oncoming blast waves. Finally, we quantitatively showed that, to different extents, both spectacles and goggles lose their effectiveness as the angle of the head orientation relative to the oncoming blast wave increases.

Acknowledgment

This research was supported by the U.S. Army Military Operational Medicine Research Program at the U.S. Army Medical Research and Materiel Command, Fort Detrick, MD. We thank the Air Force Research Laboratory, Dayton, OH, and the Army Research Laboratory, Adelphi, MD, for the use of high performance computing systems. The opinions and assertions contained herein are the private views of the authors and do not reflect the views of the U.S. Army or of the U.S. Department of Defense.

Funding Data

- Medical Research and Materiel Command (MOMRP-19780).

References

[1] Weichel, E. D., Colyer, M. H., Ludlow, S. E., Bower, K. S., and Eiseman, A. S., 2008, "Combat Ocular Trauma Visual Outcomes During Operations Iraqi and Enduring Freedom," Ophthalmology, **115**(12), pp. 2235–2245.
[2] Scott, R., 2011, "The Injured Eye," Philos. Trans. R. Soc. London B Biol. Sci., **366**(1562), pp. 251–260.
[3] Adams, G. L., 2004, "Combat Eye Protection, the FY 2005 Rapid Fielding Initiative (RFI), and the Approved Product List (APL)," U.S. Army Office of the Surgeon General and Assistant Chief, Medical Service Corps, Falls Church, VA.
[4] Cockerham, G. C., Rice, T. A., Hewes, E. H., Cockerham, K. P., Lemke, S., Wang, G., Lin, R. C., Glynn-Milley, C., and Zumhagen, L., 2011, "Closed-Eye Ocular Injuries in the Iraq and Afghanistan Wars," N. Engl. J. Med., **364**(22), pp. 2172–2173.
[5] Abbotts, R., Harrison, S. E., and Cooper, G. L., 2007, "Primary Blast Injuries to the Eye: A Review of the Evidence," J. R. Army Med. Corps, **153**(2), pp. 119–123.
[6] Hines-Beard, J., Marchetta, J., Gordon, S., Chaum, E., Geisert, E. E., and Rex, T. S., 2012, "A Mouse Model of Ocular Blast Injury That Induces Closed Globe Anterior and Posterior Pole Damage," Exp. Eye Res., **99**, pp. 63–70.
[7] Mohan, K., Kecova, H., Hernandez-Merino, E., Kardon, R. H., and Harper, M. M., 2013, "Retinal Ganglion Cell Damage in an Experimental Rodent Model of Blast-Mediated Traumatic Brain Injury," Invest. Ophthalmol. Vis. Sci., **54**(5), pp. 3440–3450.
[8] Wang, H. C., Choi, J. H., Greene, W. A., Plamper, M. L., Cortez, H. E., Chavko, M., Li, Y., Dalle Lucca, J. J., and Johnson, A. J., 2014, "Pathophysiology of Blast-Induced Ocular Trauma With Apoptosis in the Retina and Optic Nerve," Mil. Med., **179**(8S), pp. 34–40.
[9] Bhardwaj, R., Ziegler, K., Seo, J. H., Ramesh, K. T., and Nguyen, T. D., 2014, "A Computational Model of Blast Loading on the Human Eye," Biomech. Model. Mechanobiol., **13**(1), pp. 123–140.
[10] Rossi, T., Boccassini, B., Esposito, L., Clemente, C., Iossa, M., Placentino, L., and Bonora, N., 2012, "Primary Blast Injury to the Eye and Orbit: Finite Element Modeling," Invest. Ophthalmol. Vis. Sci., **53**(13), pp. 8057–8066.
[11] Bailoor, S., Bhardwaj, R., and Nguyen, T. D., 2015, "Effectiveness of Eye Armor During Blast Loading," Biomech. Model. Mechanobiol., **14**(6), pp. 1227–1237.

[12] Chandra, N., Ganpule, S., Kleinschmit, N. N., Feng, R., Holmberg, A. D., Sundaramurthy, A., Selvan, V., and Alai, A., 2012, "Evolution of Blast Wave Profiles in Simulated Air Blasts: Experiment and Computational Modeling," Shock Waves, **22**(5), pp. 403–415.
[13] Gordon, C. C., Blackwell, C. L., Bradtmiller, B., Parham, J. L., Barrientos, P., Paquette, S. P., Corner, B. D., Carson, J. M., Venezia, J. C., and Rockwell, B. M., 2014, "2012 Anthropometric Survey of U.S. Army Personnel: Methods and Summary Statistics," U.S. Army Natick Soldier Research, Development and Engineering Center, Natick, MA, DTIC Document No. ADA611869.
[14] Ganpule, S., Gu, L., Alai, A., and Chandra, N., 2012, "Role of Helmet in the Mechanics of Shock Wave Propagation Under Blast Loading Conditions," Comput. Methods Biomech. Biomed. Eng., **15**(11), pp. 1233–1244.
[15] Ellis, B., and Smith, R., 2008, *Polymers: A Property Database*, CRC Press, Boca Raton, FL.
[16] Lee, T., and Lakes, R. S., 1997, "Anisotropic Polyurethane Foam With Poisson's Ratio Greater Than 1," J. Mater. Sci., **32**(9), pp. 2397–2401.
[17] Shiina, Y., Hamamoto, Y., and Okumura, K., 2006, "Fracture of Soft Cellular Solids—Case of Non-Crosslinked Polyethylene Foam," Europhys. Lett., **76**(4), pp. 588–594.
[18] Needham, C. E., 2010, *Blast Waves*, Springer, Berlin.